"A-frame" vs. "open-book" geometries in binuclear complexes bridged by diphosphines and mercaptothiazolinate ligands. Unusual examples involving a bridging bis(diphenylphosphino)ethane group

JIANLIANG XIAO AND MARTIN COWIE[1]

Department of Chemistry, The University of Alberta, Edmonton, Alta., Canada T6G 2G2

Received November 27, 1992

JIANLIANG XIAO and MARTIN COWIE. Can. J. Chem. **71**, 726 (1993).

Reaction of the tetracarbonyl species $[M(CO)_2(\mu\text{-mtz})]_2$ (M = Rh, Ir; mtz = 2-mercaptothiazolinate) with 1 equivalent of the diphosphines ($Ph_2P(CH_2)_nPPh_2$; n = 1 (dppm), 2 (dppe)) yields the compounds $[M_2(CO)_2(\mu\text{-L})(\mu\text{-mtz})_2]$ (M = Rh, L = dppm (**1**), dppe (**3**); M = Ir, L = dppm (**2**)), which readily undergo oxidative addition of iodine to give $[M_2I_2(CO)_2(\mu\text{-L})(\mu\text{-mtz})_2]$ (M = Rh, L = dppm (**4**), dppe (**6**); M = Ir, L = dppm (**5**)). When 2 equivalents of dppm are used, the A-frame compounds $[M_2(CO)_2(\eta^1\text{-mtz})(\mu\text{-mtz})(dppm)_2]$ (M = Rh (**7**), Ir (**8**)) are afforded. In solution the dangling mtz group of **7** undergoes exchange with both the free mtz anion and the bridging mtz ligand. Compounds **7** and **8** are also produced by treatment of *trans*-$[MCl(CO)(dppm)]_2$ (M = Rh, Ir) with 2 equivalents of the mtz anion. Reaction of these dppm-bridged dichloro species with 1 equivalent of the mtz anion yields $[M_2Cl(CO)_2(\mu\text{-mtz})(dppm)_2]$ (M = Rh (**9***a*), Ir (**10**)). Compound **9***a* undergoes reversible Cl^- dissociation to give $[Rh_2(CO)_2(\mu\text{-mtz})(dppm)_2][Cl]$ (**9***b*), which is also the stable form in the solid. Reaction of **9** with CO gives the carbonyl-bridged species $[Rh_2(CO)_2(\mu\text{-CO})(\mu\text{-mtz})(dppm)_2][Cl]$. The structures of **6** and **9***b* have been determined by X-ray crystallography. Compound **6** crystallizes in the triclinic space group $P\bar{1}$ with one-half equivalent of THF per asymmetric unit in a cell having a = 9.856(3) Å, b = 14.078(6) Å, c = 16.245(5) Å, α = 103.66(3)°, β = 93.21(3)°, γ = 92.91(3)°, V = 2182(1) Å^3, and Z = 2, and has refined to R = 0.045 and R_w = 0.057 on the basis of 433 parameters varied. Compound **9***b* crystallizes with one equivalent of CH_2Cl_2 in the monoclinic space group $P2_1/n$ with a = 11.400(1) Å, b = 21.944(2) Å, c = 22.134(1) Å, β = 92.494(7)°, V = 5532(1) Å^3, and Z = 4, and has refined to R = 0.062 and R_w = 0.082 on the basis of 613 parameters varied.

JIANLIANG XIAO et MARTIN COWIE. Can. J. Chem. **71**, 726 (1993).

La réaction des espèces tétracarbonylées $[M(CO)_2(\mu\text{-mtz})]_2$ (M = Rh, Ir; mtz = 2-mercaptothiazolinate) avec un équivalent de diphosphines ($Ph_2P(CH_2)_aPPh_2$; n = 1 (dppm), 2 (dppe)) fournit les composés $[M(CO)_2(\mu\text{-L})(\mu\text{-mtz})_2]$ (M = Rh, L = dppm (**1**), dppe (**3**); M = Ir, L = dppm (**2**)), qui subissent l'addition oxydative d'iode pour donner les $[M_2I_2(CO)_2(\mu\text{-L})(\mu\text{-mtz})_2]$ (M = RH, L = dppm (**4**), dppe (**6**); M = Ir, L = dppm (**5**)). Lorsqu'on utilise deux équivalents de dppm, on obtient les composés en forme de A, $[M_2(CO)_2(\eta^1\text{-mtz})(\mu\text{-mtz})_2(dppm)_2]$ (M = Rh (**7**) et Ir (**8**)). En solution, le groupe mtz pendant du produit **7** subit un échange avec l'anion mtz libre ainsi qu'avec le coordinat mtz agissant comme pont. On obtient aussi les composés **7** et **8** par traitement du *trans*-$[MCl(CO)dppm)]_2$ (M = Rh ou Ir) avec deux équivalents de l'anion mtz. Le réaction de ces espèces dichlorées comportant un pont dppm avec un équivalent de l'anion mtz fournit les espèces $M_2Cl(CO)_2(\mu\text{-mtz})(dppm)_2]$ (M = Rh (**9***a*), Ir (**10**)). Le composé **9***a* subit une dissociation réversible du Cl^- pour donner le $[Rh_2(CO)_2(\mu\text{-mtz})(dppm)_2][Cl]$ (**9***b*) qui est aussi la forme stable à l'état solide. La réaction du produit **9** avec du CO fournit des espèces comportant un pont carbonyle $[Rh_2(CO)_2(\mu\text{-CO}(\mu\text{-mtz})(dppm)_2][Cl]$. Les structures des composés **6** et **9***b* one été déterminées par diffractions des rayons X. Le composé **6** cristallise dans le groupe d'espace triclinique $P\bar{1}$, avec un demi équivalent de THF par unité asymétrique, avec a = 9,856(3), b = 14,078(6) et c = 16,245(5) Å, α = 103,66(3)°, β = 93,21(3)° et γ = 92,91(3)°, V = 2182(1) Å^3 et Z = 2; on a affiné sa structure jusqu'à des valeurs de R = 0,045 et R_w = 0,057 pour 433 paramètres. Le composé **9***b* cristallise avec un équivalent de CH_2Cl_2 dans le groupe d'espace monoclinique $P2_1/n$ avec a = 11,400(1), b = 21,944(2) et c = 22,134(1) Å, β = 92,494(7)°, V = 5532(1) Å^3 et Z = 4; on a affiné sa structure jusqu'à des valeurs de R = 0,062 et R_w = 0,082 pour 613 paramètres.

[Traduit par la rédaction]

Introduction

Binuclear complexes, in which the metals are held in close proximity, are of interest because of the possibility that the two metals may interact in a cooperative manner and in so doing may display chemistry unique from that displayed at a single metal (1). Two common classes of binuclear complexes involving Rh and Ir are those of the "A-frame" and related compounds (2) or of the "open-book" (3) complexes. In the former class the metals are bridged by two neutral diphosphine or related groups (most often dppm ($Ph_2PCH_2PPh_2$)), occupying a *trans* orientation at each metal, whereas in the latter class the only bridging groups are anionic and occupy *cis* positions at both metals, as shown below for **A** and **B**, respectively.

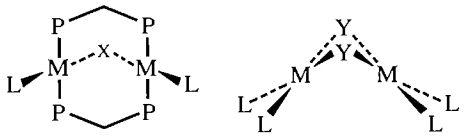

A **B**

In an effort to combine some of the features of both classes of binuclear species we set out to prepare open-book complexes that also contained bridging dppm groups. As a starting point we chose species related to the 2-mercaptothiazolinate-bridged complexes, $[M(CO)L(\mu\text{-mtz})]_2$ (M = Rh, Ir), since the dirhodium species, in which L = PMe_3, was shown to have a short metal–metal separation of ca. 3.05 Å (3*m*), comparable to the bite of dppm, suggesting that this group could be incorporated as an additional bridge in these complexes. Previous work had also shown that the mtz-

[1]Author to whom correspondence may be addressed.

bridged binuclear frameworks readily undergo fragmentation in reactions involving molecules such as H_2S and H_2.[2] It seemed likely that the incorporation of a bridging diphosphine group into these complexes would offer greater stability and may allow the isolation of open-book complexes in which one, or even both, bridging mercaptothiazolinate groups were terminally bound. Such "bridge-opened" species had been proposed as key intermediates in the activation of substrates by open-book binuclear complexes (4). We were also interested in the possibility of incorporating dppe ($Ph_2PCH_2CH_2PPh_2$) as a bridging group by utilizing an open-book complex in which the metals are constrained to be in close proximity. Complexes having this diphosphine as a bridging group are extremely rare (5) owing to the well-established propensity of this group to chelate (6). These and related studies are reported herein.

Experimental

All solvents were dried and distilled before use and were stored under dinitrogen. Reactions were carried out at room temperature by using standard Schlenk procedures. 2-Mercaptothiazoline (Hmtz) and bis(diphenylphosphino)methane (dppm) were purchased from Aldrich, bis(diphenylphosphino)ethane (dppe) was obtained from Strem Chemicals, hydrated iridium(III) chloride was obtained from Johnson–Matthey, and ^{13}CO (99%) was supplied by Isotec Inc. These and all other reagents were used as received. The compounds *trans*-$[MCl(CO)(dppm)]_2$ (M = Rh (7), Ir (8)), $[M(COD)(\mu\text{-mtz})]_2$ (M = Rh, Ir)(3*n*), and $[Rh(CO)_2(\mu\text{-mtz})]_2$ (3*m*) were prepared by the previously reported procedures.

The NMR spectra were recorded on a Bruker AM400 spectrometer at 400.1 MHz for ^1H, at 161.9 MHz for $^{31}P\{^1H\}$, and at 100.6 MHz for $^{13}C\{^1H\}$ spectra. The $^{13}C\{^1H, ^{31}P\}$ NMR spectra were obtained on a Bruker WH200 spectrometer operating at 50.32 MHz. Infrared spectra were performed on Nicolet 7199 or Mattson Polaris Fourier transform interferometers with use of Nujol mulls on KBr plates, or in solution in KCl cells with 0.5-mm window path lengths. Spectral data for all compounds are given in Table 1. Elemental analyses were performed by the microanalytical service within the department. Conductivity measurements were made on 1.0×10^{-3} M solutions with use of a Yellow Springs Instrument Co., model 31 conductivity bridge.

Preparation of compounds

(a) $[Rh_2(CO)_2(\mu\text{-mtz})_2(dppm)]$ (1)

To a THF solution of $[Rh(CO)_2(\mu\text{-mtz})]_2$, prepared by the addition of CO to a THF solution of $[Rh(COD)(\mu\text{-mtz})]_2$ (66.0 mg, 0.10 mmol, in 10 mL), was added 38.4 mg (0.10 mmol) of dppm in 5 mL of THF, causing an immediate colour change from wine red to dark purple. After stirring for 1 h, the volume was reduced to ca. 5 mL and 10 mL of hexane was slowly added to the solution, affording the compound as dark purple microcrystals (75% yield). Anal. calcd. for $Rh_2S_4P_2O_2N_2C_{33}H_{28}$: C 44.90, H 3.43, N 3.17; found: C 44.91, H 3.98, N 3.03.

(b) $[Ir_2(CO)_2(\mu\text{-mtz})_2(dppm)]$ (2)

The procedure was the same as for **1**, except that $[Ir(COD)(\mu\text{-mtz})]_2$ was used to prepare the tetracarbonyl precursor. The dark purple compound was only spectroscopically characterized due to its extreme air sensitivity.

(c) $[Rh_2(CO)_2(\mu\text{-mtz})_2(\mu\text{-dppe})]$ (3)

To a THF solution of $[Rh(CO)_2(\mu\text{-mtz})]_2$ (prepared from $[Rh(COD)(\mu\text{-mtz})]_2$ (66.0 mg, 0.10 mmol, in 10 mL of THF)) was slowly added 38.5 mg (0.097 mmol) of dppe in 5 mL of THF, causing an immediate colour change to deep red. The mixture was stirred for ca. 0.5 h and the volume was then reduced to ca. 2 mL followed by addition of hexane to give a red precipitate. This compound was extremely air sensitive, the solid instantly changing colour to brown upon exposure to air.

(d) $[Rh_2I_2(CO)_2(\mu\text{-mtz})_2(dppm)]\cdot 0.5$ THF (4)

To a THF solution of **1** (prepared from 66.0 mg (0.10 mmol) of $[Rh(COD)(\mu\text{-mtz})]_2$ (in 10 mL of THF)) was added 24.5 mg (0.097 mmol) of I_2 in 4 mL of THF, causing an immediate colour change from intense purple to dark red. After stirring for 1 h, the volume was reduced to ca. 2 mL, and addition of hexane precipitated a dark red solid (70% yield). Anal. calcd. for $Rh_2I_2S_4P_2O_{2.5}N_2C_{35}H_{32}$: C 35.84, H 2.93, N 2.39, I 21.65; found: C 35.61, H 2.85, N 2.31, I 21.80.

(e) $[Ir_2I_2(CO)_2(\mu\text{-mtz})_2(dppm)]$ (5)

To a THF solution of **2** (prepared by using $[Ir(COD)(\mu\text{-mtz})]_2$ (84.0 mg, 0.10 mmol, in 10 mL of THF)) was added 24.5 mg (0.097 mmol) of I_2 in 4 mL of THF, causing an immediate colour change to orange. The mixture was stirred for 0.5 h, after which reduction of the volume followed by addition of hexane precipitated an orange solid.

(f) $[Rh_2I_2(CO)_2(\mu\text{-mtz})_2(\mu\text{-dppe})]\cdot 0.5$ THF (6)

To a THF solution of **3** (prepared from 134.0 mg (0.20 mmol) of $[Rh(COD)(\mu\text{-mtz})]_2$) was added 51.0 mg of I_2 in 5 mL of THF; a deep purple solution was immediately formed. Reduction of the volume followed by addition of hexane yielded a dark red solid (70–75% yield). The solid was stored overnight under vacuum. Anal. calcd. for $Rh_2I_2S_4P_2O_{2.5}N_2C_{36}H_{36}$: C 36.44, H 3.06, N 2.36, I 21.39; found: C 36.80, H 3.18, N 2.29, I 22.66. The presence of THF was verified by NMR and the X-ray study (*vide infra*).

(g) $[Rh_2(mtz)(CO)_2(\mu\text{-mtz})(dppm)_2]\cdot CH_2Cl_2$ (7)

Method A. To a THF solution of $[Rh(CO)_2(\mu\text{-mtz})]_2$ (prepared from $[Rh(COD)(\mu\text{-mtz})]_2$ (132.0 mg, 0.2 mmol, in 20 mL)) was added 153.0 mg (0.40 mmol) of dppm, resulting in an immediate colour change to deep red. After stirring for 0.5 h, the volume was reduced to ca. 5 mL followed by precipitation with hexane. Compound **7** was crystallized from CH_2Cl_2–hexane. Anal. calcd. for $Rh_2Cl_2S_4P_4O_2N_2C_{59}H_{54}$: C 52.41, H 4.03, N 2.07, S 9.49; found: C 52.85, H 3.95, N 2.20, S 9.70.

Method B. A 110.0 mg (0.10 mmol) sample of *trans*-$[RhCl(CO)(dppm)]_2$ was suspended in 10 mL of THF, to which was added 28.4 mg (0.20 mmol) of sodium-2-mercaptothiazolinate in 5 mL of THF, causing a colour change to red within several min. After stirring for 5 h, the solvent was removed under vacuum. The red solid was redissolved in 10 mL of CH_2Cl_2. The solution was then filtered and concentrated to ca. 3 mL. Microcrystals were obtained upon addition of hexane (90% yield).

(h) $[Ir_2(mtz)(CO)_2(\mu\text{-mtz})(dppm)_2]$ (8)

To a slurry of *trans*-$[IrCl(CO)(dppm)]_2$ (220.0 mg, 0.17 mmol) in 10 mL of THF was added 49.0 mg (0.34 mmol) of sodium-2-mercaptothiazolinate in 5 mL of THF. The mixture was stirred overnight, during which time a red-orange solution was formed. Filtration followed by reduction in the volume of the solution and addition of hexane gave an orange solid (85–90% yield). Anal. calcd. for $Ir_2S_4P_4O_2N_2C_{58}H_{52}$: C 48.18, H 3.63, N 1.94; found: C 47.83, H 3.70, N 2.03.

(i) $[Rh_2(CO)_2(\mu\text{-mtz})(dppm)_2][Cl]\cdot CH_2Cl_2$ (9b)

The procedure was the same as for **7** in method B, except that 1 equivalent of sodium-2-mercaptothiazolinate was used. Red crystals of **9*b*** were obtained from CH_2Cl_2-hexame (87% yield). Conductivity measurements: $\Lambda = 29.8\ \Omega^{-1}\ cm^2\ mol^{-1}$ in CH_2Cl_2; $\Lambda = 71.6\ \Omega^{-1}\ cm^2\ mol^{-1}$ in CH_3NO_2. Anal. calcd. for $Rh_2Cl_3S_2P_4O_2NC_{56}H_{50}$: C 52.99, H 3.99, N 1.10; found: C 52.97, H 3.95, N 1.01.

(j) $[Rh_2(CO)_2(\mu\text{-mtz})(dppm)_2][PF_6]$ (9c)

To a CH_2Cl_2 solution of **9*b*** (118.0 mg, 0.10 mmol, in 10 mL) was added 1 equivalent of $AgPF_6$ (25.0 mg, 0.10 mmol, in 5 mL of CH_2Cl_2). After stirring for 0.5 h, the solution was filtered and the volume was then reduced to ca. 3 mL. Microcrystals were obtained upon addition of hexane (90% yield). Anal. calcd. for

[2] J. Xiao and M. Cowie, unpublished results.

TABLE 1. Spectroscopic data[a]

	IR, cm^{-1}		NMR[d]		
	Solid[b]	Solution[c]	$\delta(^{31}P\{^1H\})$[e]	$\delta(^{13}C\{^1H\})$[f]	$\delta(^1H)$[f]
$[Rh_2(CO)_2(dppm)$-$(\mu\text{-}mtz)_2]$ (**1**)	1995 (vs), 1948 (vs)[g]		45.9 (dd, $^1J_{Rh-P}$ = 142.8 Hz, $^2J_{P-P}$ = 58.2 Hz), 30.8 (dd, $^1J_{Rh-P}$ = 153.4 Hz)		4.20 (m, 1H), 3.70 (m, 1H), 4.28 (m, 2H), 3.80 (m, 1H), 3.41 (m, 1H), 3.33 (m, 1H), 3.06 (m, 1H), 2.94 (m, 2H)
$[Ir_2(CO)_2(dppm)$-$(\mu\text{-}mtz)_2]$ (**2**)	1962 (vs, br)		−5.7 (m), −2.8 (m)		5.20 (m, 1H), 4.18 (m, 1H), 4.38 (m, 1H), 3.55 (m, 2H), 3.40 (m, 2H), 3.20 (m, 1H), 2.20 (m, 1H), 2.00 (m, 1H)
$[Rh_2(CO)_2(dppe)$-$(\mu\text{-}mtz)_2]$ (**3**)		1980 (st), 1960 (med)[g]	40.2 (dd, $^1J_{Rh-P}$ = 147.6 Hz, $^3J_{P-P}$ = 2.6 Hz), 39.1 (dd, $^1J_{Rh-P}$ = 157.8 Hz)		4.20 (m 1H), 3.73 (m, 1H), 2.37 (m, 1H), 1.80 (m, 1H), 4.16 (m, 1H), 3.34 (m, 1H), 3.23 (m, 1H), 3.10 (m, 2H), 2.98 (m, 1H), 2.70 (m, 1H), 2.32 (m, 1H)
$[Rh_2I_2(CO)_2(dppm)$-$(\mu\text{-}mtz)_2]$ (**4**)	2059 (st) 2037 (med)	2062 (st), 2020 (med)	19.2 (m), 18.6 (m)	189.2 (dd, $^1J_{Rh-C}$ = 55.6 Hz, $^2J_{P-C}$ = 7.7 Hz), 186.0 (dd, $^1J_{Rh-C}$ = 56.6 Hz, $^2J_{P-C}$ = 7.7 Hz)	5.20 (m, 1H), 4.15 (m, 1H), 5.06 (m, 1H), 4.08 (m, 2H), 3.90 (m, 1H), 3.32 (m, 1H), 3.20 (m, 1H), 2.94 (m, 1H), 2.10 (m, 1H)
$[Ir_2I_2(CO)_2(dppm)$-$(\mu\text{-}mtz)_2]$ (**5**)	2039 (vs), 2018 (med)	2034 (vs, br)	−26.1 (d, $^2J_{P-P}$ = 37.8 Hz), −21.5 (d)		4.98 (m, 1H), 4.01 (m, 1H), 4.52 (m, 1H), 3.89 (m, 2H), 3.80 (m, 1H), 3.34 (m, 1H), 3.10 (m, 1H), 2.87 (m, 1H), 2.02 (m, 1H)
$[Rh_2I_2(CO)_2(dppe)$-$(\mu\text{-}mtz)_2]$ (**6**)	2062 (st), 2025 (med)	2062 (st), 2020 (med)	40.9 (d, $^1J_{Rh-P}$ = 109.2 Hz), 22.3 (d, $^1J_{Rh-P}$ = 110.0 Hz)		2.42 (m, 1H), 2.30 (m, 1H), 2.20 (m, 1H), 1.97 (m, 1H), 5.32 (m, 1H), 4.32 (m, 1H), 3.96 (m, 1H), 3.69 (m, 1H), 3.37 (m, 1H), 3.32 (m, 1H), 3.25 (m, 1H), 2.85 (m, 1H)
$[Rh_2(CO)_2(\eta^1\text{-}mtz)$-$(\mu\text{-}mtz)(dppm)_2]$ (**7**)[h]	1926 (st), 1825 (w, br)	2000 (vs), 1973 (st), 1936 (vs, br), 1820 (w, br)	31.4 (br), 24.5 (br)	205.3 (br), 195.0 (br)	4.32 (m, 4H), 3.78 (m, 2H), 3.15 (t, 2H), 2.70 (t, 2H), 1.83 (t, 2H)
$[Ir_2(CO)_2(\eta^1\text{-}mtz)$-$(\mu\text{-}mtz)(dppm)_2]$ (**8**)	1946 (w), 1896 (st)	1952 (st, br), 1893 (vs, br)	4.5 (m), −6.9 (m)	186.3 (t, $^2J_{P-C}$ = 14.6 Hz), 180.6 (br)	4.93 (m, 2H), 4.26 (m, 2H), 4.41 (t, 2H), 3.30 (t, 2H), 2.68 (t, 2H), 1.67 (t, 2H)
$[Rh_2(CO)_2(\mu\text{-}mtz)$-$(dppm)_2][Cl]$ (**9***b*)	1988 (vs), 1953 (vs)	2001 (vs), 1970 (st, br)	30.1 (m), 20.6 (m)	194.4 (dt, $^1J_{Rh-C}$ = 67 Hz, $^2J_{P-C}$ = 12 Hz), 193.4 (dt, $^1J_{Rh-C}$ = 75 Hz, $^2J_{P-C}$ = 15 Hz)	3.94 (m, 2H), 3.84 (m, 2H), 2.39 (t, 2H), 1.46 (t, 2H)
$[Rh_2(CO)_2(\mu\text{-}mtz)(dppm)_2]$-$[PF_6]$ (**9***c*)	1991 (vs), 1952 (vs)	2001 (vs), 1977 (st)	29.0 (m), 20.7 (m)		3.63 (m, 2H), 3.75 (m, 2H), 2.35 (t, 2H), 1.36 (t, 2H)
$[Ir_2Cl(CO)_2(\mu\text{-}mtz)$-$(dppm)_2]$ (**10**)	1944 (st), 1893 (vs)	1960 (med), 1902 (vs)	5.4 (m), −5.8 (m)		4.88 (m, 2H), 4.18 (m, 2H), 2.56 (t, 2H), 1.98 (t, 2H)
$[Rh_2(CO)_2(\mu\text{-}CO)$-$(\mu\text{-}mtz)(dppm)_2]$ [Cl] (**11***a*)	1981 (st), 1958 (vs), 1797 (st)	1985 (vs, br), 1812 (st)	32.2 (m), 30.8 (m)		4.22 (m, 2H), 4.12 (m, 2H), 3.00 (t, 2H), 1.86 (t, 2H)

TABLE 1 (*concluded*)

	IR, cm^{-1}		NMR[d]		
	Solid[b]	Solution[c]	$\delta(^{31}P\{^1H\})$[e]	$\delta(^{13}C\{^1H\})$[f]	$\delta(^1H)$[f]
$[Rh_2(CO)_2(\mu\text{-}CO)(\mu\text{-}mtz)(dppm)_2][PF_6]$ (**11***b*)	1976 (vs, br), 1798 (st)	1987 (vs, br), 1813 (st)	32.4 (m), 30.9 (m)		4.25 (m, 2H), 3.95 (m, 2H), 3.02 (t, 2H), 1.88 (t, 2H)

[a]Abbreviations used: d = doublet, t = triplet, m = multiplet, dd = doublet of doublets, dt = doublet of triplets, br = broad, w = weak, med = mesium, st = strong, vs = very strong.
[b]Nujol mull.
[c]THF solution except compounds **7**, **9**, and **11**, CH_2Cl_2 solution.
[d]CD_2Cl_2 solution at 25°C, except compound **3**, in THF-d_8, and compounds **9***b*, *c*, at −80°C.
[e]Versus 85% H_3PO_4.
[f]Versus TMS.
[g]ν(CO).
[h]See text.

$Rh_2ClS_2P_5F_6O_2NC_{55}H_{48}$: C 49.69, H 3.65, N 1.05; found: C 49.56, H 3.64, N 1.14.

*(k) [$Ir_2Cl(CO)_2(\mu\text{-}mtz)(dppm)_2$] (**10**)*

The procedure was the same as for **8**, except that 1 equivalent of sodium-2-mercaptothiazolinate was used. Compound **10** was crystallized from THF–hexane. Anal. calcd. for $Ir_2ClS_2P_4O_2NC_{55}H_{48}$: C 48.47, H 3.56, N 1.03; found: C 48.63, H 3.90, N 0.91.

*(l) [$Rh_2(CO)_2(\mu\text{-}CO)(\mu\text{-}mtz)(dppm)_2$][Cl] (**11**a)*

A stream of CO was passed through a CH_2Cl_2 solution of **9**, causing an immediate colour change to orange accompanied by formation of an orange precipitate. Carbonyl loss from **11***a* occurred very rapidly under dinitrogen. Compound **11***a* was determined to be a 1:1 electrolyte in CH_3NO_2 (Λ = 74.0 Ω^{-1} cm^2 mol^{-1}).

*(m) [$Rh_2(CO)_2(\mu\text{-}CO)(\mu\text{-}mtz)(dppm)_2$][$PF_6$] (**11**b)*

The procedure was the same as for **11***a*, except that **9***c* was used. Carbonyl loss from **11***b* also occurred very readily.

X-ray data collection

*(a) [$Rh_2I_2(CO)_2(\mu\text{-}mtz)_2(dppe)$]·0.5 THF (**6**)*

Dark red crystals of **6** were grown by diffusion of hexane into a THF solution of the complex. Suitable crystals were mounted on glass fibres with use of epoxy cement. Data were collected on an Enraf–Nonius CAD4 diffractometer using MoKα radiation. Unit-cell parameters were obtained from a least-squares refinement of the setting angles of 25 reflections in the range $12.6 \leq 2\theta \leq 33.6°$. The automatic peak search and reflection indexing programs[3] generated a triclinic cell with the possible space groups of $P1$ or $P\bar{1}$. The space group $P\bar{1}$ was chosen, and later verified by the successful refinement of the structure.

Intensity data were collected at 22°C by using the $\theta/2\theta$ scan technique to a maximum $2\theta = 50°$. Backgrounds were scanned for 25% of the peak width on either side of the peak scan. Three reflections were chosen as intensity standards, being remeasured after every 120 min of X-ray exposure; no unusual variation in their intensities was evident. The data were processed in the usual manner with a value of 0.04 for p to downweigh intense reflections (9). Corrections for Lorenz and polarization effects and for absorption by using the method of Walker and Stuart were applied (10).

*(b) [$Rh_2(CO)_2(\mu\text{-}mtz)(dppm)_2$][Cl]·$CH_2Cl_2$ (**9**b)*

Red crystals of **9***b* were obtained by diffusion of hexane into a CH_2Cl_2 solution of the complex. Crystals were mounted and flame-sealed in glass capillaries under solvent vapour to minimize solvent loss. Data collection and derivation of unit-cell parameters proceeded in a manner similar to that above (the setting angles of 25 reflections were in the range $22.0° \leq 2\theta \leq 25.7°$). The monoclinic diffraction symmetry and systematic absences ($h0l$, $h + l$ = odd; $0k0$, k = odd) were consistent with the space group $P2_1/n$.

Intensity data were collected at 22°C with use of the $\theta/2\theta$ scan technique to a maximum $2\theta = 50.0°$. No unusual variation was found for the intensity standards. See Table 2 for pertinent crystal data and details of intensity collection for both **6** and **9***b*.

Structure solution and refinement

Both structures were solved in the respective space groups ($P\bar{1}$ for **6** and $P2_1/n$ for **9***b*) with use of standard Patterson and Fourier techniques. Full-matrix least-squares refinements proceeded so as to minimize the function $\Sigma w(|F_o| - |F_c|)^2$, where $w = 4F_o^2/\sigma^2(F_o^2)$. Atomic scattering factors and anomalous dispersion terms were taken from the usual tabulations, refs. 11–13. The positions of all hydrogen atoms in the complex were generated on the basis of the geometry of their attached carbon atom with C—H distances of 0.95 Å. Thermal parameters for the hydrogens were fixed at 1.2 times that of their attached carbon atom. The hydrogen atoms were included as fixed contributions in the least-squares calculations. The solvent atoms of complex **6** were input as a rigid half-occupancy five-carbon ring that most appropriately described the ring of poorly resolved, smeared-out electron density that appeared on Fourier maps. The occupancy of $\frac{1}{2}$ was established by ^1H NMR of the crystals and the thermal parameters of 12 $Å^2$ were arbitrarily selected since these atoms were not well behaved in refinement attempts; they were not refined in subsequent least-squares cycles, and their hydrogen atoms were not included. Due to the bad disorder of the THF molecule the carbon and oxygen atoms could not be distinguished so were all input as carbon atoms.

The final model for complex **6**, with 433 parameters varied, refined to $R = 0.045$ and $R_w = 0.057$. In the final difference Fourier map the 10 highest residuals had intensities of 0.8–1.1 e $Å^{-3}$ and were primarily located near the disordered solvent molecule. For compound **9***b* the final model, with 613 parameters varied, converged to $R = 0.062$ and $R_w = 0.082$. The 10 highest peaks (0.6–2.5 e $Å^{-3}$) were again located near the solvent molecule. There is apparently some slight disorder of the mtz^- ligand as seen by the larger thermal parameters of S(2) and C(7); however, this was not resolvable. The positional and thermal parameters for the non-hydrogen atoms, excluding the phenyl groups, of **6** are given in Table 3, and selected bond lengths and angles are given in Tables 5 and 6, respectively. For complex **9***b* the pertinent data are found in Tables 4, 7, and 8. Anisotropic thermal parameters, idealized hydrogen parameters, and bond lengths and angles within the phenyl

[3]Programs used were those of the Enraf–Nonius Structure Determination Package, in addition to local programs by R. G. Ball.

TABLE 2. Summary of crystal data and details of intensity collection

Compound	$[Rh_2I_2(CO)_2(\mu\text{-mtz})_2(dppe)]\cdot 0.5$ THF (**6**)	$[Rh_2(CO)_2(\mu\text{-mtz})(dppm)_2][Cl]\cdot CH_2Cl_2$ (**9***b*)
Formula	$C_{36}H_{36}I_2N_2O_{2.5}P_2Rh_2S_4$	$C_{56}H_{50}Cl_3NO_2P_4Rh_2S_2$
fw	1186.52	1269.22
Space group	$P\bar{1}$	$P2_1/n$
Temp, °C	22	22
Radiation (λ, Å)	Graphite-monochromated MoKα (0.71069)	
Cell parameters		
a, Å	9.856(3)	11.400(1)
b, Å	14.078(6)	21.944(2)
c, Å	16.245(5)	22.134(1)
α, deg	103.66(3)	
β, deg	93.21(3)	92.494(7)
γ, deg	92.91(3)	
V, Å^3	2182(3)	5532(1)
Z	2	4
ρ(calcd.), g/cm^3	1.806	1.524
No. of unique data collected	7606 (h, $\pm k$, $\pm l$)	9932 (h, k, $\pm l$)
No. of unique data used ($F_o^2 \geq 3\sigma(F_o^2)$)	5164	6170
Final no. of parameters refined	433	613
R	0.045	0.062
R_w	0.057	0.082

$R = \Sigma||F_o| - |F_c||/\Sigma|F_o|$.
$R_w = (\Sigma w(|F_o| - |F_c|)^2/\Sigma w|F_o|^2)^{1/2}$.

rings and solvent molecules for **6** and **9***b* are available as supplementary data.[4]

Discussion

Previous studies (3*m*,*n*) have shown that the 2-mercaptothiazolinate ion (mtz$^-$), diagrammed below, coordinates to two metal centres through the mercapto sulfur and the nitrogen atom. The complexes of Rh and Ir so-formed have

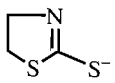

typical open-book structures. Although the tetracarbonyl species $[Rh(CO)_2(\mu\text{-mtz})]_2$ has been described (3*m*), the diiridium analogue $[Ir(CO)_2(\mu\text{-mtz})]_2$ was not previously reported. Both are prepared by the reaction of their cyclooctadiene precursors, $[M(COD)(\mu\text{-mtz})]_2$ (3*n*) with CO in THF. Neither species was isolated but each was reacted *in situ* with the appropriate phosphine to obtain the desired product. The IR spectrum of the diiridium tetracarbonyl precursor displays the expected carbonyl bands (2075, 2040, 2005, and 1990 cm^{-1}) typical of these open-book complexes (3*j*,*l*,*m*).

A series of mtz-bridged complexes of rhodium, containing monodentate tertiary phosphines such as PPh_3, has been described (3*m*); however, no complex involving this anionic bridging group and diphosphine ligands such as $Ph_2PCH_2PPh_2$ (dppm) has been reported. As was the case for monodentate phosphines, these tetracarbonyl species react readily with the diphosphine, dppm, yielding the dppm-bridged products, $[M_2(CO)_2(dppm)(\mu\text{-mtz})_2]$ (M = Rh(**1**), Ir(**2**)), as shown below. For the rhodium species **1** the two carbonyl stretches in the IR spectrum (1995, 1948 cm^{-1}) display a significantly larger separation than those of the PPh_3 analogue (1974, 1966 cm^{-1}). This is probably a consequence of the geometrical difference in these two species. In the PPh_3 adduct the phosphines have a *trans* disposition at the two metals and both carbonyl groups are opposite the nitrogen ends of the bridging mtz ligands (3*m*). In **1**

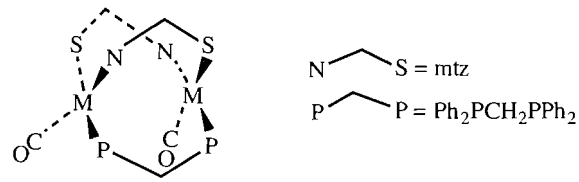

M = Rh (**1**); Ir (**2**)

and **2**, however, the bridging dppm group demands that the ends of the diphosphine group be mutually *cis*, so assuming a head-to-tail arrangement of mtz ligands, one carbonyl will be *trans* to nitrogen while the other is opposite sulfur. A head-to-tail arrangement, in which different ends of the two ligands are bound to each metal, is most often seen in binuclear complexes containing these anionic three-atom bridges (3*b*,*g*,*h*,*k*,*l*), although the head-to-head arrangement has also been reported (3*j*). The bifunctional nature of the mtz ligands in **1** gives rise to two chemically inequivalent phosphorus nuclei (also opposite either N or S) as shown in the $^{31}P\{^1H\}$ NMR spectrum, which displays two doublets of doublets at δ 30.8 ($^1J_{RhP}$ = 153.4 Hz, $^2J_{PP}$ = 58.2 Hz) and δ 45.9 ($^1J_{RhP}$ = 142.8 Hz). The geometry observed leads to the inequivalence of all 10 methylene protons associated with the dppm and mtz groups, although owing to overlap of two of these resonances in the ^1H NMR spectrum only nine are

[4]A complete set of data may be purchased from: The Depository of Unpublished Data, Document Delivery, CISTI, National Research Council Canada, Ottawa, Canada K1A 0S2.

Tables of hydrogen atom parameters and bond lengths and angles have also been deposited with the Cambridge Crystallographic Data Centre and can be obtained on request from The Director, Cambridge Crystallographic Data Centre, University of Chemical Laboratory, 12 Union Road, Cambridge CB2 1EZ, U.K.

TABLE 3. Positional and thermal parameters of the atoms of $[Rh_2I_2(CO)_2(\mu\text{-mtz})_2(\mu\text{-dppe})]\cdot 0.5THF$ (**6**)[a]

Atom	*x*	*y*	*z*	*B* (Å^2)
I(1)	0.05272(6)	0.27594(5)	0.49247(4)	4.10(2)
I(2)	−0.04596(6)	0.24254(5)	−0.02031(4)	4.23(2)
Rh(1)	0.06825(6)	0.26932(4)	0.32039(4)	2.32(1)
Rh(2)	0.04262(6)	0.26163(4)	0.14957(4)	2.29(1)
S(1)	0.1953(2)	0.4219(1)	0.3365(1)	2.84(5)
S(2)	0.1022(3)	0.5931(2)	0.2780(2)	4.78(7)
S(3)	−0.1984(2)	0.2637(2)	0.1703(2)	3.78(6)
S(4)	−0.3236(2)	0.4296(2)	0.2825(2)	6.28(9)
P(1)	0.2595(2)	0.1801(1)	0.3199(1)	2.66(5)
P(2)	0.2691(2)	0.2727(2)	0.1160(1)	2.57(5)
O(1)	−0.1215(7)	0.0878(5)	0.3003(5)	5.6(2)
O(2)	0.0142(7)	0.0441(4)	0.1132(4)	4.7(2)
N(1)	0.0546(6)	0.4152(4)	0.1872(4)	2.6(2)
N(2)	−0.1046(6)	0.3553(5)	0.3286(4)	2.9(2)
C(1)	−0.0503(9)	0.1557(7)	0.3056(5)	3.7(2)
C(2)	0.0287(8)	0.1269(6)	0.1274(5)	3.2(2)
C(3)	0.3543(7)	0.1630(5)	0.2250(5)	2.9(2)
C(4)	0.3891(7)	0.2584(5)	0.1999(5)	2.7(2)
C(5)	0.1107(8)	0.4653(6)	0.2574(5)	2.8(2)
C(6)	0.028(1)	0.5798(7)	0.1778(7)	6.4(4)
C(7)	−0.0102(9)	0.4758(6)	0.1396(6)	4.3(3)
C(8)	−0.1955(8)	0.3465(7)	0.2674(6)	3.7(2)
C(9)	−0.253(1)	0.4822(8)	0.3870(7)	5.6(3)
C(10)	−0.1238(9)	0.4393(7)	0.3977(6)	4.7(3)

[a]Numbers in parentheses are estimated standard deviations in the least significant digits in this and all subsequent tables. All atoms shown were refined anisotropically. Thermal parameters for the anisotropically refined atoms are given in the form of the equivalent isotropic displacement parameters defined as $4/3[a^2\beta_{11} + b^2\beta_{22} + c^2\beta_{33} + ab(\cos\gamma)\beta_{12} + ac(\cos\beta)\beta_{13} + bc(\cos\alpha)\beta_{23}]$. Atoms of solvent molecule of crystallization and of the phenyl carbons are given as supplementary material.

TABLE 4. Positional and thermal parameters of the atoms of $[Rh(CO)_2(\mu\text{-mtz})(dppm)_2][Cl]\cdot CH_2Cl_2$ (**9***b*)[a]

Atom	*x*	*y*	*z*	*B* (Å^2)
Rh(1)	0.11508(6)	0.25121(3)	0.15107(3)	2.51(2)
Rh(2)	0.25220(6)	0.36751(3)	0.16145(3)	2.50(2)
Cl(1)	0.5878(3)	0.1926(2)	0.9490(1)	7.5(1)
S(1)	0.3954(2)	0.2938(1)	0.1995(1)	3.23(6)
S(2)	0.4559(2)	0.1667(1)	0.2336(1)	4.76(8)
P(1)	0.0518(2)	0.2647(1)	0.2493(1)	2.98(6)
P(2)	0.2012(2)	0.3801(1)	0.2610(1)	2.66(5)
P(3)	0.1864(2)	0.2297(1)	0.0556(1)	2.71(6)
P(4)	0.3179(2)	0.3516(1)	0.0648(1)	2.81(6)
O(1)	−0.0506(6)	0.3452(3)	0.1024(3)	4.7(2)
O(2)	0.1887(7)	0.4958(3)	0.1332(4)	6.0(2)
N(1)	0.2497(6)	0.1963(3)	0.1889(3)	2.8(2)
C(1)	0.0109(8)	0.3065(5)	0.1202(4)	3.4(2)
C(2)	0.2069(9)	0.4453(5)	0.1430(4)	3.8(3)
C(3)	0.1582(7)	0.3078(4)	0.2947(4)	2.6(2)
C(4)	0.3241(7)	0.2710(4)	0.0448(3)	2.5(2)
C(5)	0.3502(8)	0.2193(4)	0.2039(4)	3.0(2)
C(6)	0.2485(9)	0.1298(5)	0.1976(4)	4.3(3)
C(7)	0.344(1)	0.1110(6)	0.2395(7)	7.4(4)

[a]See footnote of Table 3.

resolved (Table 1). The methylene resonances for the dppm group (δ 4.20, 3.70) were identified by the appropriate ^{31}P-decoupling experiments. The spectroscopic parameters for **2** are comparable to those of **1**, suggesting similar structures.

Although these species have been identified as open-book species having a bridging dppm group, they can also be viewed as A-frame complexes having the dppm and one of the mtz groups in mutually *trans* bridging positions and the other mtz group in the apical position opposite the carbon-

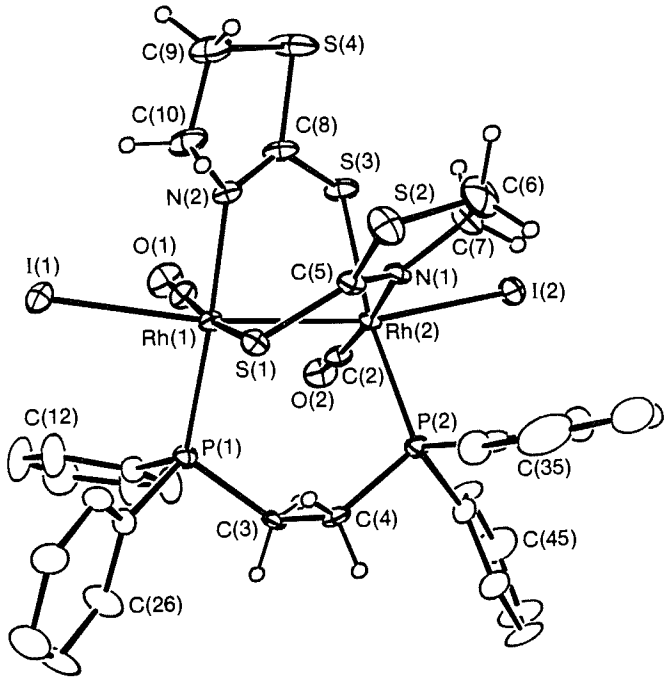

FIG. 1. A representation of $[Rh_2I_2(CO)_2(\mu\text{-mtz})_2(\mu\text{-dppe})]$ (**6**) showing the numbering scheme. Thermal ellipsoids are shown at the 20% probability level except for methylene hydrogens, which are artifically small. Phenyl hydrogens are not shown.

TABLE 5. Selected distances (Å) in $[Rh_2I_2(CO)_2(\mu\text{-dppe})(\mu\text{-mtz})_2]\cdot 0.5$ THF (**6**)

Rh(1)—Rh(2)	2.748 (1)	Rh(1)—I(1)	2.788 (1)
Rh(1)—S(1)	2.382 (2)	Rh(1)—P(1)	2.317 (2)
Rh(1)—N(2)	2.132 (5)	Rh(1)—C(1)	1.892 (7)
Rh(2)—I(2)	2.794 (1)	Rh(2)—S(3)	2.418 (2)
Rh(2)—P(2)	2.333 (2)	Rh(2)—N(1)	2.099 (5)
Rh(2)—C(2)	1.842 (7)	S(1)—C(5)	1.737 (6)
S(3)—C(8)	1.724 (7)	S(2)—C(5)	1.758 (6)
S(2)—C(6)	1.712 (8)	S(4)—C(8)	1.754 (7)
S(4)—C(9)	1.772 (8)	P(1)—C(3)	1.821 (6)
P(1)—C(11)	1.820 (7)	P(1)—C(21)	1.829 (6)
P(2)—C(4)	1.809 (6)	P(2)—C(31)	1.806 (7)
P(2)—C(41)	1.816 (7)	O(1)—C(1)	1.139 (8)
O(2)—C(2)	1.133 (7)	N(1)—C(5)	1.270 (7)
N(1)—C(7)	1.430 (8)	N(2)—C(8)	1.280 (8)
N(2)—C(10)	1.453 (8)	C(3)—C(4)	1.522 (8)
C(6)—C(7)	1.47 (1)	C(9)—C(10)	1.453 (9)

yls. In these compounds, with three similar bridging groups, the A-frame and open-book formulations are clearly two equivalent ways of categorizing the same structure.

Reaction of $[Rh(CO)_2(\mu\text{-mtz})]_2$ with 1 equivalent of dppe ($Ph_2PCH_2CH_2PPh_2$) yields $[Rh_2(CO)_2(\mu\text{-dppe})(\mu\text{-mtz})_2]$ (**3**), an unusual example of a dppe-bridged species, analogous to compounds **1** and **2**. This species is extremely air sensitive and was only characterized spectroscopically. Its IR spectrum shows two carbonyl stretches like those of the dppm analogue **1**, and its $^{31}P\{^1H\}$ NMR spectrum shows two resonances, at δ 39.1 ($^1J_{RhP}$ = 157.8 Hz, $^3J_{PP}$ = 2.6 Hz) and δ 40.2 ($^1J_{RhP}$ = 147.6 Hz). Although the 3-bond P–P coupling is much smaller than that observed in other dppe-bridged complexes such as $[WM(CO)_{10}(dppe)]$ (M = Cr, Mo, W), for which values of ca. 35 Hz are observed (14), it is comparable to the results obtained for $[Ru_4H_4(CO)_{10}(\mu\text{-dppe})]$, for which no P–P coupling was observed (15).

The ^1H NMR spectrum of **3** resembles those of **1** and **2**, suggesting a structure similar to the dppm analogues, as shown. The four resonances (δ 4.20, 3.73, 2.37, 1.80) assigned to the dppe methylene groups were identified by

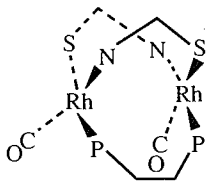

3

broad-band ^{31}P decoupling.

One of the unique reactivity patterns of binuclear compounds is the transannular oxidative-addition reaction, which results in a formal one-electron oxidation of each metal, often accompanied by metal–metal bond forming or breaking (*3a,e,i,l*). Although each of the monophosphine complexes $[M(CO)(PR_3)(\mu\text{-mtz})]_2$ (M = Rh; Ir; R = Ph, Me) gives mixtures of several species in the reactions with halogens (footnote 2), all three diphosphine-bridged species **1–3** readily undergo transannular oxidative addition of I_2 to cleanly yield the respective products **4–6**, diagrammed below. These three oxidized products are more stable than their M(+1) precursors, permitting the isolation of the dppe-bridged **6**, and allowing unambiguous confirmation of the bridging dppe group. In these three products the IR spectra show two carbonyl stretches, the frequencies of which have increased by ca. 70 cm^{-1} from those of the precursors, as expected for the oxidation of the metals from the +1 to the +2 oxidation state. The $^{31}P\{^1H\}$ NMR spectra for all three compounds are consis-

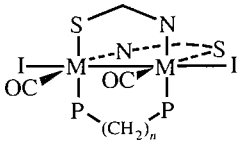

M = Rh, *n* = 1 (**4**); *n* = 2 (**6**)
= Ir, *n* = 1 (**5**)

tent with two chemically different phosphorous environments, one opposite sulfur and the other opposite nitrogen. For **4** the Rh–P and P–P couplings are not immediately obvious owing to the complexity of the spectrum; however, for **5** and **6** the $^{31}P\{^1H\}$ spectra are simple, both appearing as two sets of doublets, resulting from two-bond phosphorus–phosphorus coupling in **5** and one-bond rhodium–phosphorus coupling in **6**. No P–P coupling is resolved in the spectrum of **6**. Other spectral parameters, shown in Table 1, are in agreement with these structural formulations, which have been verified by the X-ray structure determination of **6**.

The structure of $[Rh_2I_2(CO)_2(\mu\text{-mtz})_2(\mu\text{-dppe})]$ (**6**) is shown in Fig. 1, and the associated structural parameters are summarized in Tables 5 and 6. This determination clearly confirms the binuclear, dppe-bridged structure, in which the two mtz ligands bridge in a head-to-tail arrangement. In this geometry the complex can again be viewed as an open-book complex bridged by dppe or it can be thought of as resembling an A-frame complex, except with rather substantial distortions resulting from the small bite of the mtz ligands combined with the wide bite of the dppe group. In this latter

TABLE 6. Selected angles (deg) in $[Rh_2I_2(CO)_2(\mu\text{-mtz})_2(\mu\text{-dppe})]\cdot 0.5$ THF (**6**)

I(1)—Rh(1)—Rh(2)	171.61 (2)	I(1)—Rh(1)—S(1)	97.51 (5)
I(1)—Rh(1)—P(1)	89.21 (5)	I(1)—Rh(1)—N(2)	87.8 (1)
I(1)—Rh(1)—C(1)	83.6 (2)	Rh(2)—Rh(1)—S(1)	86.73 (5)
Rh(2)—Rh(1)—P(1)	97.72 (5)	Rh(2)—Rh(1)—N(2)	85.4 (1)
Rh(2)—Rh(1)—C(1)	91.4 (2)	S(1)—Rh(1)—P(1)	94.29 (6)
S(1)—Rh(1)—N(2)	84.5 (1)	S(1)—Rh(1)—C(1)	173.5 (2)
P(1)—Rh(1)—N(2)	176.6 (1)	P(1)—Rh(1)—C(1)	92.1 (2)
N(2)—Rh(1)—C(1)	89.2 (3)	I(2)—Rh(2)—Rh(1)	166.88 (2)
I(2)—Rh(2)—S(3)	83.22 (6)	I(2)—Rh(2)—P(2)	90.54 (5)
I(2)—Rh(2)—N(1)	97.6 (1)	I(2)—Rh(2)—C(2)	87.3 (2)
Rh(1)—Rh(2)—S(3)	84.09 (6)	Rh(1)—Rh(2)—P(2)	102.38 (5)
Rh(1)—Rh(2)—N(1)	85.3 (1)	Rh(1)—Rh(2)—C(2)	89.3 (2)
S(3)—Rh(2)—P(2)	172.03 (7)	S(3)—Rh(2)—N(1)	88.3 (1)
S(3)—Rh(2)—C(2)	89.6 (2)	P(2)—Rh(2)—N(1)	87.6 (1)
P(2)—Rh(2)—C(2)	95.0 (2)	N(1)—Rh(2)—C(2)	174.3 (3)
Rh(1)—S(1)—C(5)	99.8 (2)	C(5)—S(2)—C(6)	89.2 (3)
Rh(2)—S(3)—C(8)	100.3 (2)	C(8)—S(4)—C(9)	90.1 (3)
Rh(1)—P(1)—C(3)	116.2 (2)	Rh(1)—P(1)—C(11)	113.8 (2)
Rh(1)—P(1)—C(21)	118.5 (2)	C(3)—P(1)—C(11)	103.7 (3)
C(3)—P(1)—C(21)	99.1 (3)	C(11)—P(1)—C(21)	103.4 (3)
Rh(2)—P(2)—C(4)	113.3 (2)	Rh(2)—P(2)—C(31)	112.1 (2)
Rh(2)—P(2)—C(41)	121.3 (2)	C(4)—P(2)—C(31)	107.3 (3)
C(4)—P(2)—C(41)	98.1 (3)	C(31)—P(2)—C(41)	103.1 (3)
Rh(2)—N(1)—C(5)	124.5 (4)	Rh(2)—N(1)—C(7)	123.6 (4)
C(5)—N(1)—C(7)	111.7 (5)	Rh(1)—N(2)—C(8)	123.0 (4)
Rh(1)—C(1)—O(1)	177.1 (6)	Rh(2)—C(2)—O(2)	177.0 (6)
P(1)—C(3)—C(4)	113.0 (4)	P(2)—C(4)—C(3)	110.1 (4)
S(1)—C(5)—S(2)	115.7 (3)	S(1)—C(5)—N(1)	127.4 (5)
S(2)—C(5)—N(1)	116.9 (5)	S(2)—C(6)—C(7)	109.8 (5)
N(1)—C(7)—C(6)	110.6 (6)	S(3)—C(8)—S(4)	117.5 (4)
S(3)—C(8)—N(2)	125.7 (5)	S(4)—C(8)—N(2)	116.8 (5)
S(4)—C(9)—C(10)	108.0 (5)	N(2)—C(10)—C(9)	112.5 (6)

formulation the dppe and mtz groups, which are mutually *trans*, take the positions occupied by dppm groups in the majority of A-frames, while the other mtz ligand occupies the apical site opposite the carbonyls. Both iodo ligands occupy the positions on each metal opposite the Rh—Rh bond, giving the metals octahedral geometries. The Rh—Rh separation of 2.748(1) Å is consistent with a single bond, as expected between the two Rh(II) centres. The octahedra are offset from each other in two ways. First they are inclined about the axial directions (parallel to the Rh–P vectors) by a dihedral angle of 16.4° owing to the differing bites of the mtz and dppe groups, as noted. These different bites are clearly seen in the N(2)–S(3) and P(1)–P(2) non-bonded separations of 2.685(6) and 3.841(3) Å, respectively. Second, the octahedra are staggered about the Rh—Rh bond by an average torsion angle of ca. 33°. Although this skewing may be required to minimize nonbonded contacts between the carbonyl groups, it is more likely necessary in order to accommodate the bridging dppe ligand. A similar twisting of the metal framework has been observed in dppe-bridged complexes of rhenium in which torsion angles up to 50° have been noted (16).

Most parameters within the complex are normal, therefore the Rh—P distances (2.317(2), 2.333(2) Å) are in good agreement, and resemble the analogous distances in dppm-bridged complexes. The Rh—S and Rh—N distances are also normal, except that the distances for atoms opposite dppe are longer than those opposite the carbonyls (Rh—S = 2.418(2), 2.382(2) Å; Rh—N = 2.132(5), 2.099(5) Å). This is the opposite of that observed in the related species $[Rh(CO)(PPh_3)(\mu\text{-SPh})]_2$, in which the Rh—S bonds opposite phosphorus were found to be shorter than those opposite CO (17).

Unlike diphosphine bridges, which are generally rather inert, the mercaptothiazolinate bridges are quite labile and are readily broken (footnote 2). It was therefore of interest to determine whether both mtz bridges would remain intact upon reaction with two equivalents of dppm. Given the overwhelming preference of dppm to bridge metals, and the unlikelihood that both dppm *and* both mtz ligands would simultaneously bridge, it was anticipated that one or both mtz ligands might move from their bridging sites. Treatment of $[M(CO)_2(\mu\text{-mtz})]_2$ (M = Rh, Ir) with two equivalents of dppm yields $[M_2(CO)_2(\eta^1\text{-mtz})(\mu\text{-mtz})(dppm)_2]$ (M = Rh(**7**), Ir(**8**)) as diagrammed below. The diiridium species **8** displays two signals in the $^{31}P\{^1H\}$ NMR spectrum, characteristic of an AA′BB′ spin system, and shows four resonances in the ^1H NMR spectrum for the mtz methylene hydrogens at δ 4.41, 3.30, 2.68, and 1.67, in addition to the dppm resonances. Based on a comparison with the resonances for the free mtz anion, at δ 4.0 and 3.6, the low-field resonances above are attributed to the dangling group, while the high-field pair are identified as those of the bridging group. The dangling mtz ligand, as shown, is proposed to coordinate through sulfur as has been suggested for closely related ligands in other complexes (*3h*, 18). In the IR spectrum of **8** the two carbonyl bands (1946, 1896 cm^{-1}) are consistent with terminally bound carbonyls, although the lower frequency stretch suggests that this may result from a weak semi-bridging interaction with the second metal, as is demonstrated for **7** (*vide infra*). The $^{13}C\{^1H\}$ NMR spectrum

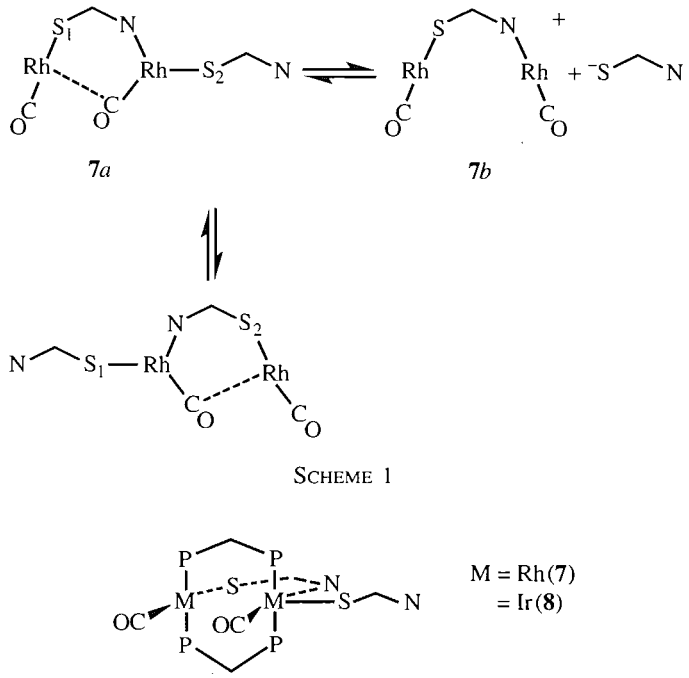

SCHEME 1

M = Rh(7)
= Ir(8)

displays two sharp triplets for the carbonyls at −70°C, the high-field one of which becomes broad and featureless at room temperature, without changing significantly in position. The reason for the broadening is not obvious.

In contrast to **8**, the NMR spectra of **7** show strong temperature dependence, and its solution IR spectrum is more complicated than expected for a dicarbonyl. In the solid the IR spectrum of **7** displays the two carbonyl bands expected at 1926 and 1825 cm^{-1}; again the low-frequency band is suggestive of a semibridging mode as shown for structure **7***a* in Scheme 1. However, in solution, four carbonyl stretches are observed. The lower frequency pair (1936, 1820 cm^{-1}), which are close to those of the solid, appear to correspond to **7***a* while those at 2000 and 1973 cm^{-1} appear to arise from the cationic species **7***b*, which results from mercaptothiazolinate ion dissociation. Addition of excess mtz^- (as the sodium salt) supports this proposed equilibrium, causing a decrease in the intensity of the two high-frequency bands and an increase in those ascribed to **7***a*. This equilibrium is also apparent in the NMR spectra. At ambient temperature the mtz protons appear in the ^1H NMR spectrum at δ 4.32, 3.15, 2.70, and 1.83. As excess mtz^- is added to a solution of **7**, the two low-field resonances increase in intensity and shift towards the resonances for free mtz^- (δ 4.0, 3.6). Not only does this behaviour support the previous assignment for the mtz proton resonances in **8**, it also supports the equilibrium between **7***a* and **7***b*. At −80°C resonances due to both **7***a* (δ 32.5, 26.5) and **7***b* (δ 29.5, 20.8) are observed in the $^{31}P\{^1H\}$ NMR spectrum, in an approximate 4:1 intensity ratio, respectively. This assignment is based on the close resemblance of the spectral parameters of the minor species (**7***b*) with those of the cationic species, $[Rh_2(CO)_2(\mu\text{-mtz})(dppm)_2][X]$ (X = Cl(**9***b*), PF_6(**9***c*)) (*vide infra*). In the $^{13}C\{^1H\}$ NMR spectrum of **7** at −80°C the resonance at δ 193.3 ($^1J_{RhC}$ = 74.6 Hz, $^2J_{PC}$ = 16 Hz) is assigned to the terminal carbonyl of **7***a* and the broad doublet at δ 211.8 is ascribed to the semibridging carbonyl of this species. Broadband ^{31}P decoupling experiments clearly show this semibridging interaction, as the ^{13}C resonance transforms from a broad doublet to a doublet of doublets with 67 Hz coupling to one rhodium and 13 Hz coupling to the other. The signals arising from the carbonyls of the minor species (**7***b*) are apparently obscured by the high-field ^{13}C resonance of **7***a*, as indicated by the broadness of the bottom part of the latter as well as by its integration. In the ^1H NMR spectrum at −80°C the appearance of a major and minor species in the appropriate ratio is also apparent, although a couple of the resonances for the major species shift substantially, and some of those for the minor species are obscured by other resonances. Selective homonuclear decoupling experiments at ambient temperature point to an additional fluxionality that occurs slowly on the NMR time scale. Irradiation of one of the methylene proton resonances of the bridging mtz group causes the other methylene resonance of this group to collapse to a singlet, as expected. However, unexpectedly this results in a significant decrease in the intensity of the corresponding methylene resonance of the dangling group. This observation of spin saturation transfer indicates a slow exchange of terminal and bridging mtz groups as diagrammed vertically in Scheme I. Attempts to increase the rate of terminal-bridging mtz exchange to achieve rapid interconversion, by raising the temperature, were unsuccessful since the compound decomposed at temperatures above ca. 45°C.

TABLE 7. Selected distances (Å) in $[Rh_2(CO)_2(\mu\text{-mtz})(dppm)_2]$-$[Cl]\cdot CH_2Cl_2$ (**9***b*)

Rh(1)—P(1)	2.339 (2)	Rh(1)—P(3)	2.346 (2)
Rh(1)—N(1)	2.097 (5)	Rh(1)—C(1)	1.811 (7)
Rh(2)—S(1)	2.422 (2)	Rh(2)—P(2)	2.320 (2)
Rh(2)—P(4)	2.324 (2)	Rh(2)—C(2)	1.824 (7)
S(1)—C(5)	1.719 (6)	S(2)—C(5)	1.775 (6)
S(2)—C(7)	1.78 (1)	P(1)—C(3)	1.809 (6)
P(1)—C(11)	1.801 (6)	P(1)—C(21)	1.838 (7)
P(2)—C(3)	1.829 (6)	P(2)—C(31)	1.836 (6)
P(2)—C(41)	1.826 (6)	P(3)—C(4)	1.838 (6)
P(3)—C(51)	1.820 (6)	P(3)—C(61)	1.840 (7)
P(4)—C(4)	1.824 (6)	P(4)—C(71)	1.848 (6)
P(4)—C(81)	1.837 (6)	O(1)—C(1)	1.159 (7)
O(2)—C(2)	1.147 (8)	N(1)—C(5)	1.283 (7)
N(1)—C(6)	1.472 (8)	C(6)—C(7)	1.46 (1)

Complexes containing two bridging dppm groups and a bridging mtz ligand can also be obtained by the reactions of *trans*-$[MCl(CO)(dppm)]_2$ (M = Rh, Ir) with sodium mercaptothiazolinate. When two equivalents of mtz^- are used, compounds **7** and **8** are obtained, as seen in the reactions of $[M(CO)_2(\mu\text{-mtz})]_2$ with two equivalents of dppm. When the above dppm-bridged dichloro complexes are reacted with only one equivalent of mtz^-, replacement of only one chloride ligand occurs, yielding $[M_2Cl(CO)_2(\mu\text{-mtz})(dppm)_2]$ (M = Rh(**9**), Ir(**10**)). The spectral parameters for **10** are closely comparable to those of **8**, apart from the absence of resonances for the dangling mtz group in the ^1H NMR spectrum, so this compound is assigned an analogous structure in which the dangling mtz group in **8** is replaced by a terminal chloro ligand in **10**.

Although **9** is shown above as having a coordinated chloro ligand, in solution it, like compound **7**, is better represented as an equilibrium mix of the neutral species **9***a* together with the cationic species **9***b*, resulting from chloride dissociation as shown in eq. [1]. This is clearly seen in the IR spectrum

TABLE 8. Selected angles (deg) in $[Rh_2(CO)_2(\mu\text{-mtz})(dppm)_2][Cl]\cdot CH_2Cl_2$ (**9***b*)

P(1)—Rh(1)—P(3)	174.96(6)	P(1)—Rh(1)—N(1)	87.3 (1)
P(1)—Rh(1)—C(1)	92.4 (2)	P(3)—Rh(1)—N(1)	88.1 (1)
P(3)—Rh(1)—C(1)	92.4 (2)	N(1)—Rh(1)—C(1)	172.9 (2)
S(1)—Rh(2)—P(2)	86.69 (6)	S(1)—Rh(2)—P(4)	88.86 (6)
S(1)—Rh(2)—C(2)	151.9 (2)	P(2)—Rh(2)—P(4)	175.27 (6)
P(2)—Rh(2)—C(2)	91.2 (2)	P(4)—Rh(2)—C(2)	92.0 (2)
Rh(2)—S(1)—C(5)	117.1 (2)	C(5)—S(2)—C(7)	89.7 (3)
Rh(1)—P(1)—C(3)	110.9 (2)	Rh(1)—P(1)—C(11)	120.9 (2)
Rh(1)—P(1)—C(21)	110.5 (2)	C(3)—P(1)—C(11)	107.2 (3)
C(3)—P(1)—C(21)	104.5 (3)	C(11)—P(1)—C(21)	101.3 (3)
Rh(2)—P(2)—C(3)	111.5 (2)	Rh(2)—P(2)—C(31)	113.3 (2)
Rh(2)—P(2)—C(41)	118.6 (2)	C(3)—P(2)—C(31)	103.7 (3)
C(3)—P(2)—C(41)	103.8 (3)	C(31)—P(2)—C(41)	104.4 (3)
Rh(1)—P(3)—C(4)	110.4 (2)	Rh(1)—P(3)—C(51)	117.8 (2)
Rh(1)—P(3)—C(61)	116.6 (2)	C(4)—P(3)—C(51)	107.0 (3)
C(4)—P(3)—C(61)	102.1 (3)	C(51)—P(3)—C(61)	101.3 (3)
Rh(2)—P(4)—C(4)	112.7 (2)	Rh(2)—P(4)—C(71)	112.9 (2)
Rh(2)—P(4)—C(81)	119.4 (2)	C(4)—P(4)—C(71)	102.5 (3)
C(4)—P(4)—C(81)	103.1 (3)	C(71)—P(4)—C(81)	104.4 (3)
Rh(1)—N(1)—C(5)	120.5 (4)	Rh(1)—N(1)—C(6)	127.7 (4)
C(5)—N(1)—C(6)	111.7 (5)	Rh(1)—C(1)—O(1)	174.9 (6)
Rh(2)—C(2)—O(2)	173.6 (6)	P(1)—C(3)—P(2)	114.3 (3)
P(3)—C(4)—P(4)	113.9 (3)	S(1)—C(5)—S(2)	116.1 (3)
S(1)—C(5)—N(1)	128.8 (5)	S(2)—C(5)—N(1)	115.1 (5)
N(1)—C(6)—C(7)	110.7 (6)	S(2)—C(7)—C(6)	106.1 (6)

[1] $[Rh_2Cl(CO)_2(\mu\text{-mtz})(dppm)_2]$ (**9***a*)

$$\rightleftharpoons [Rh_2(CO)_2(\mu\text{-mtz})(dppm)_2][Cl] \text{ (9}b\text{)}$$

in solution, which displays three carbonyl stretches at 2001, 1970, and 1933 cm^{-1}. The middle band is broad and apparently results from two overlapping bands, so the stretches due to **9***a* appear at 1970 and 1933 cm^{-1} whereas those of **9***b* appear at 2001 and 1970 cm^{-1}. Addition of $AgBF_4$ to solutions of **9** results in the disappearance of the 1933 cm^{-1} band and sharpening of the central band, and addition of sodium chloride causes these bands to reappear. In the solid state the two carbonyl bands observed (1988, 1953 cm^{-1}) are consistent with the ionic structure **9***b*, and this is confirmed by an X-ray structure determination of this species (*vide infra*).

As was noted for **7***a* and **7***b*, the exchange between **9***a* and **9***b* is fast on the NMR time scale. Thus at ambient temperature both the $^{31}P\{^1H\}$ and the $^{13}C\{^1H\}$ NMR spectra of the equilibrium mixture display two broad resonances, while the ^1H NMR spectrum shows only two triplets (δ 2.43, 1.85) for the mtz methylene protons. Lowering the temperature sharpens the signals in the $^{31}P\{^1H\}$ and $^{13}C\{^1H\}$ NMR spectra. However, in contrast to the equilibrium involving **7***a* and **7***b*, only one species is revealed at −80°C, the spectroscopic parameters of which closely resemble those of $[Rh_2(CO)_2(\mu\text{-mtz})(dppm)_2][PF_6]$ (**9***c*) obtained by reaction of **9** with $AgPF_6$. Therefore it is clear that lowering the temperature shifts the equilibrium in favor of **9***b*. At −80°C, the $^{31}P\{^1H\}$ NMR spectrum of **9***b* is as expected for an unsymmetric structure, and the $^{13}C\{^1H\}$ NMR spectrum reveals two doublets of triplets at δ 194.4 and 193.4, reminiscent of those of **7***b*. The mtz methylene hydrogens appear as triplets at δ 2.39 and 1.46.

Among the dppm-bridged binuclear compounds of group VIII metals, complexes **7–10** represent a new type of A-frames, in which the anionic capping ligand is bifunctional, binding to the two metals by different atom types, and because of this the two metal centres in these A-frames are electronically different, which could give rise to interesting reactivity patterns. The bifunctional feature of the apical mtz ligand also provides an easy access to coordinative unsaturation through cleavage from a metal of one of its ends, which is shown to be feasible by the dynamic behavior of **7**. Coordinative unsaturation induced by bridge opening has been proposed to be crucial in substrate activation by open-book compounds (4), as noted earlier. Related A-frame complexes of group VIII metals, in which the anionic apical ligands are those typically used as bridges in open-book compounds, have been reported recently (2*e*,*f*,*i*,*j*). However, these ligands, such as pyrazolyl groups, have the same atom type binding to each metal.

The structure of **9***b*, as the methylene chloride solvate, has been determined and a representation of the cation is shown in Fig. 2. This compound much more resembles conventional "A-frames" than does **6**, in that the *trans*-bridging groups are dppm with the anionic group (mtz^-) at the apex opposite the carbonyls. In fact the structure quite closely resembles that of $[Rh_2(CO)_2(\mu\text{-dmpz})(dppm)_2]^+$ (2*j*), (dmpz = 3,5-dimethylpyrazolate). The structure determination clearly shows that the chloride ion is not associated with the complex, and the closest contact between rhodium and this anion is 6.842(2) Å. Similarly the CH_2Cl_2 molecule is isolated from both the anion and the cation. Although the geometries about the Rh centres are essentially square planar, there are significant distortions from the idealized geometry. Therefore the N(1)—Rh(1)—C(1) angle is 172.9(2)° and the S(1)—Rh(2)—C(2) angle is 151.9(2)°, resulting from an apparent movement of C(1)O(1) towards Rh(2) and C(2)O(2) away from Rh(1). This distortion is accompanied by a Rh(1)—Rh(2) separation of 2.9957(7) Å, which is compressed slightly compared with the intraligand P–P nonbonded contacts of 3.056(2) and

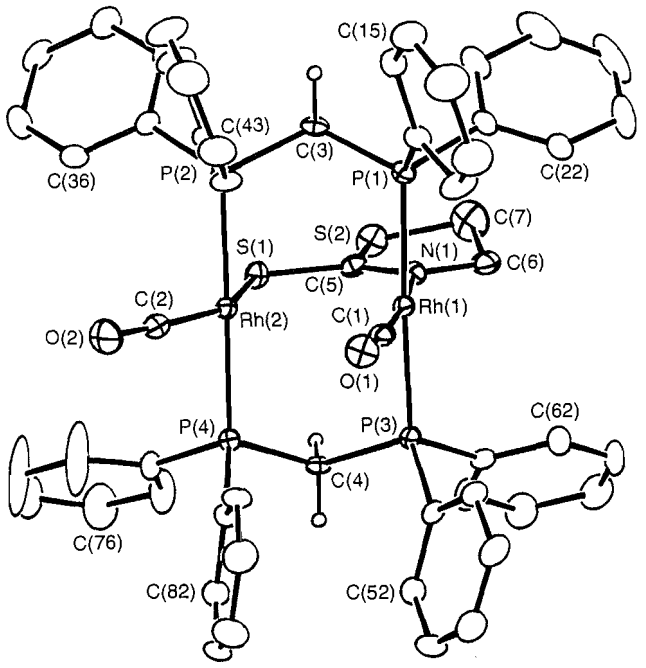

FIG. 2. A representation of the $[Rh_2(CO)_2(\mu\text{-mtz})(dppm)_2]^+$ cation of **9***a*. Thermal ellipsoids are as in Fig. 1.

3.068(2) Å, suggesting a possible weak interaction between the metals. We believe, however, that these distortions result from the packing. As can be seen in Fig. 2, phenyl rings 4 and 8 are aimed between the carbonyls and the short C(2)—H(42) and C(2)—H(86) contacts of 2.72 and 2.62 Å appear to distort this carbonyl from its idealized position. Similarly rings 1 and 5 appear to force C(1)O(1) towards Rh(2), giving a C(1)—H(12) contact of 2.56 Å. The contact between Rh(2) and C(1) (3.158(6) Å) appears to be too long to suggest even a weak semi-bridging interaction, and the IR spectra also do not argue in favor of such an interaction.

In conventional A-frames (2*a*–*c*) the capping ligand binds to both metals through a common atom, resulting in a substantial tilt of the two metal square planes by about 83°. In **9***b* (and in **6**) the capping mtz ligand binds through two well-separated donor atoms, opening up the A-frame and resulting in more closely parallel coordination planes at the metals (the dihedral angle is only 16(2)°). As such, the structure of **9***b* takes on a geometry similar to the face-to-face dimers such as *trans*-$[Rh_2Cl_2(CO)_2(dppm)_2]$ (19) and $[Rh_2(CNR)_4(dppm)_2]^{2+}$ (20, 21).

All other parameters within the complex are essentially as expected, comparing well with the appropriate parameters in **6**, so deserve no further comment.

The equilibrium mix of **9***a* and **9***b* reacts with CO to give $[Rh_2(CO)_2(\mu\text{-mtz})(\mu\text{-CO})(dppm)_2][Cl]$ (**11***a*), whereas **11***b*, having PF_6^- as the counterion, is obtained by the analogous reaction of **9***c*. Carbonyl loss from both species to give the starting complexes is very facile, occurring simply under an N_2 purge. The $^{31}P\{^1H\}$ NMR spectra of the two compounds are similar and appear as sharp AA'BB'XY spin patterns, consistent with the structure as shown. The infrared spectrum of **11***a* displays two terminal carbonyl stretches (1981, 1958 cm^{-1}), whereas for **11***b* only one stretch (1976 cm^{-1}) is revealed for the terminal carbonyls. However, the broadness of this stretch suggests that another band is beneath it. Both compounds display bridging carbonyl stretches at ca. 1797 cm^{-1} in the IR spectra. The CO stretches of **11***a*, *b* appear at significantly lower frequencies than those (2005–1860 cm^{-1}) observed for the closely related compounds, $[Rh_2(CO)_2(\mu\text{-X})(\mu\text{-CO})(dppm)_2][X]$ (X = Cl, Br, I) (19), suggesting that the mtz ligand is more electron releasing than the halides.

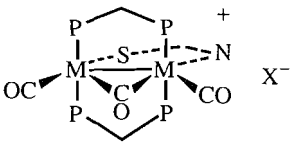

X = Cl(**11***a*); PF_6(**11***b*)

Summary

A series of binuclear complexes of Rh and Ir has been synthesized, in which the metals are bridged by both neutral diphosphine ligands (dppm and dppe) and anionic mercaptothiazolinate (mtz) groups. In the first class, $[M_2(CO)_2(\mu\text{-mtz})_2(\mu\text{-L})]$ (L = diphosphine), containing two anionic bridging groups, the complexes can be classified as having either "open-book" or "A-frame" geometries, and both descriptions appear to be equally valid. Two of these species, $[Rh_2(CO)_2(\mu\text{-mtz})_2(\mu\text{-dppe})]$ and $[Rh_2I_2(CO)_2(\mu\text{-mtz})_2(\mu\text{-dppe})]$, are unusual examples in which dppe functions as a *bridging* group. In the second class of compounds, $[M_2X(CO)_2(\mu\text{-mtz})(dppm)_2]$ (M = Rh, Ir; X = Cl, mtz), containing two bridging dppm groups, the ease of displacement of the anionic groups from a bridging site has been demonstrated. These species have only one mtz group bridging the metals and are best viewed as classical A-frame complexes. The additional anionic ligand (Cl^- or mtz^-) is terminally bound to one metal, and for M = Rh these terminal groups readily dissociate, yielding cationic complexes.

Although numerous open-book complexes containing phosphine ligands are known, the complexes $[M_2(CO)_2(\mu\text{-mtz})_2(\mu\text{-L})]$ are the first examples in which diphosphines have been incorporated as ligands together with a bifunctional ligand, binding through different atom types (S,N). It will be of interest to further explore the chemistry of these species. The complexes of the second class are interesting in that they contain a bifunctional apical ligand, the possible effects of which have been noted. It may be the bifunctionality of the mtz ligand that gives rise to the unusual dynamic behavior for the complex $[Rh_2(\eta^1\text{-mtz})(CO)_2(\mu\text{-mtz})(dppm)_2]$, as shown in Scheme 1.

Acknowledgments

We thank the Natural Sciences and Engineering Research Council of Canada (NSERC) and the University of Alberta for support of this work and NSERC for partial support of the diffractometer. We are grateful to Drs. Bernie Santarsiero and Bob McDonald of the X-ray Structure Determination Laboratory of this department for data collection on com-

pound **6**, and assistance in the final stages of refinement and data presentation.

1. (*a*) R. Poilblanc. Inorg. Chim. Acta, **62**, 75 (1982); (*b*) M. H. Chisholm. *In* Reactivity of metal–metal bonds. *Edited by* M. H. Chisholm. ACS Symp. Ser. **155**, 17 (1981); (*c*) E. L. Muetterties and J. Stein. Chem. Rev. **79**, 479 (1979).
2. (*a*) C. P. Kubiak and R. Eisenberg. Inorg. Chem. **19**, 2726 (1980); (*b*) C. P. Kubiak, C. Woodcock, and R. Eisenberg. Inorg. Chem. **19**, 2733 (1980); (*c*) M. Cowie and S. K. Dwight. Inorg. Chem. **18**, 2700 (1979); (*d*) B. A. Vaartstra, J. Xiao, J. A. Jenkins, R. Verhagen, and M. Cowie. Organometallics, **10**, 2708 (1991); (*e*) L. J. Tortorelli, C. Woods, and A. T. McPhail. Inorg. Chem. **29**, 2726 (1990); (*f*) C. Woods, L. J. Tortorelli, D. P. Rillema, J. L. E. Burn, and J. C. DePriest. Inorg. Chem. **28**, 1673 (1989); (*g*) B. A. Vaartstra and M. Cowie. Inorg. Chem. **28**, 3138 (1989); (*h*) J. A. Jenkins, J. P. Ennett, and M. Cowie. Organometallics, **7**, 1845 (1988); (*i*) D. Carmona, L. A. Oro, P. L. Pérez, A. Tiripicchio, and M. Tiripicchio-Camellini. J. Chem. Soc. Dalton Trans. 1427 (1989); (*j*) L. A. Oro, D. Carmona, P. L. Pérez, M. Esteban, A. Tiripicchio, and M. Tiripicchio-Camellini. J. Chem. Soc. Dalton Trans. 973 (1985); (*k*) B. R. Sutherland and M. Cowie. Organometallics, **4**, 1637 (1985); (*l*) R. J. Puddephatt. Chem. Soc. Rev. **12**, 98 (1983).
3. (*a*) M. T. Pinillos, A. Elduque, J. A. López, F. J. Lahoz, and L. A. Oro. J. Chem. Soc. Dalton Trans. 1391 (1991); (*b*) M. A. Ciriano, J. J. Pérez-Torrente, L. A. Oro, A. Tiripicchio, and M. Tiripicchio-Camellini. J. Chem. Soc. Dalton Trans. 255 (1991); (*c*) J. A. Bailey, S. L. Grundy, and S. R. Stobart. Organometallics, **9**, 536 (1990); (*d*) D. Carmona, F. J. Lahoz, L. A. Oro, J. Reyes, and M. P. Lamata. J. Chem. Soc. Dalton Trans. 3551 (1990); (*e*) M. T. Pinillos, A. Elduque, L. A. Oro, F. J. Lahoz, F. Bonati, A. Tiripicchio, and M. Tiripicchio-Camellini. J. Chem. Soc. Dalton Trans. 989 (1990); (*f*) G. S. Rodman and A. J. Bard. Inorg. Chem. **29**, 4699 (1990); (*g*) D. C. Boyd, R. Szalapski, and K. R. Mann. Organometallics, **8**, 790 (1989); (*h*) M. A. Ciriano, F. Viguri, J. J. Perez-Torrente, F. J. Lahoz, L. A. Oro, A. Tripicchio, and M. Tiripicchio-Camellini. J. Chem. Soc. Dalton Trans. 25 (1989); (*i*) R. B. Brost and S. R. Stobart. J. Chem. Soc. Chem. Commun. 498 (1989); (*j*) M. A. Ciriano, B. E. Villarroya, L. A. Oro, M. C. Apreda, C. Foces-Foces, and F. H. Cano. J. Organomet. Chem. **366**, 377 (1989); (*k*) G. S. Rodman and K. R. Mann. Inorg. Chem. **27**, 3338 (1988); (*l*) M. A. Ciriano, S. Sebastián, L. A. Oro, A. Tiripicchio, M. Tiripicchio-Camellini, and F. J. Lahoz. Angew. Chem. Int. Ed. Engl. **27**, 402 (1988); (*m*) M. Cowie and T. Sielisch. J. Organomet. Chem. **348**, 241 (1988); (*n*) T. Sielisch and M. Cowie. Organometallics, **7**, 707 (1988), and refs. therein.
4. (*a*) A. Dedieu, P. Escaffre, J. M. Frances, Ph. Kalck, and A. Thorez. Nouv. J. Chim. **10**, 631 (1986); (*b*) M. El Amane, R. Mathieu, and R. Poilblanc. Organometallics, **2**, 1618 (1983).
5. A. C. Price and R. A. Walton. Polyhedron, **6**, 729 (1987).
6. D. M. A. Minahan, W. E. Hill, and C. A. McAuliffe. Coord. Chem. Rev. **55**, 31 (1984).
7. J. T. Mague and J. P. Mitchener. Inorg. Chem. **8**, 199 (1969).
8. B. R. Sutherland and M. Cowie. Inorg. Chem. **23**, 2324 (1984).
9. R. J. Doedens and J. A. Ibers. Inorg. Chem. **6**, 204 (1967).
10. N. Walker and D. Stuart. Acta Crystallogr. Sect. A: Found. Crystallogr. **A39**, 158 (1983).
11. D. T. Cromer and J. T. Waber. International tables for crystallography. Vol. IV. Kynoch Press, Birmingham. 1974. Table 2.2A.
12. R. F. Stewart, E. R. Davidson, and W. T. Simpson. J. Chem. Phys. **42**, 3175 (1965).
13. D. T. Cromer and D. Liberman. J. Chem. Phys. **53**, 1891 (1970).
14. R. L. Keiter, S. L. Kaiser, N. P. Hansen, J. W. Brodack, and L. W. Cary. Inorg. Chem. **20**, 283 (1981).
15. M. R. Churchill, R. A. Lashewycz, J. R. Shapley, and S. I. Richter. Inorg. Chem. **19**, 1277 (1980).
16. (*a*) P. E. Fanwick, D. R. Root, and R. A. Walton. Inorg. Chem. **25**, 4832 (1986); (*b*) F. A. Cotton, G. G. Stanley, and R. A. Walton. Inorg. Chem. **17**, 2099 (1978).
17. J. J. Bonnet, Ph. Kalck, and R. Poilblanc. Inorg. Chem. **16**, 1514 (1977).
18. (*a*) E. S. Peterson, D. P. Bamcroft, D. Min, F. A. Cotton, and E. H. Abbott. Inorg. Chem. **29**, 229 (1990); (*b*) M. A. Ciriano, J. J. Perez-Torrente, F. Viguri, F. J. Lahoz, L. A. Oro, A. Tiripicchio, and M. Tiripicchio-Camellini. J. Chem. Soc. Dalton Trans. 1493 (1990).
19. M. Cowie and S. K. Dwight. Inorg. Chem. **19**, 2500 (1980).
20. A. L. Balch. J. Am. Chem. Soc. **98**, 8049 (1976).
21. J. T. Mague and S. H. DeVries. Inorg. Chem. **19**, 3743 (1980).